Critical state and instability locus of a silty-sand iron tailing

État critique et lieu d'instabilité d'un résidu de fer limoneux-sable

António Viana da Fonseca & Diana Cordeiro
CONSTRUCT-GEO, Faculdade de Engenharia da Universidade do Porto (FEUP), Portugal, viana@fe.up.pt

ABSTRACT: Mine waste material generated during the mining process, specifically tailings, can be used in a variety of engineering projects, most widely applied to embankment dams. Mostly dominated by fine particle size and deposition in a very loose state with a high-water content, tailings are susceptible to liquefaction under diverse static and cyclic triggering mechanisms. Recent tailings dam failures have highlighted the brittleness of these structures. This paper presents the mechanical behaviour of a silty-sand iron tailing and the analysis of liquefaction within a critical state framework, using the triaxial apparatus as reference. Isotropically consolidated strain-controlled triaxial tests allowed the definition of a critical state line (CSL) in a p'-q and p'-e plane, using the best available practices. However, a proper consideration of the undrained behaviour should be based on tests that adopt the correct initial stress state and specific stress paths as it would happen in situ. Therefore, non-conventional, anisotropically consolidated, undrained triaxial test were performed with strain paths replicating static loading. The occurrence of instability was examined using the proposed framework, for both contractive and dilative behaviour under various stress levels.

RÉSUMÉ : Les résidus de déchets miniers déchets générés pendant le processus d'extraction peuvent être utilisés dans une variété de projets d'ingénierie, le plus largement appliqués aux barrages en remblai. Principalement dominés par la granulométrie fine et le dépôt dans un état très lâche avec une teneur élevée en eau, les résidus sont susceptibles de se liquéfier sous divers mécanismes de déclenchement statiques et cycliques. Les ruptures récentes des barrages de résidus ont mis en évidence la fragilité de ces structures. Cet article présente le comportement mécanique d'un résidu de fer silteux-sable et l'analyse de la liquéfaction dans un cadre d'état critique, en utilisant l'appareil triaxial comme référence. Les essai triaxiaux contrôlés en déformation isotropiquement consolidés ont permis de définir une ligne d'état critique (CSL) dans un plan p'-q et p'-e, en utilisant les meilleures pratiques disponibles. Cependant, une prise en compte appropriée du comportement non drainé doit être basée sur des essai qui adoptent l'état de contrainte initial correct et des chemins de contraintes spécifiques tels qu'ils se produiraient in situ. Par conséquent, des essais triaxiaux non conventionnels, consolidés anisotropiquement et non drainés ont été réalisés avec des chemins de déformation répliquant la charge statique. L'occurrence de l'instabilité a été examinée à l'aide du cadre proposé, tant pour le comportement contractuel que dilatant sous différents niveaux de stress.

KEYWORDS: Tailings, Laboratory tests, Critical State Line, Liquefaction.

1 INTRODUCTION

Tailings are the by-products after the mining processes to extract the valuable fractions from ores. The most common method to dispose of the tailings is impounding a slurred material within a tailing dam. There are three basic types of tailings dams: downstream, upstream, and centerline (Carrier 2003). The upstream construction is the most popular type of embankment for tailings dams, as it is a low-cost process despite of being a high-risk operation. The upstream dams are particularly susceptible to liquefaction under seismic ground motion and the dam stability is endangered if the raising rate of the dam is high due to excess pore pressure built within the deposit during construction (Schnaid et al. 2007). Within the entire range of failure modes that have occurred at tailings impoundments, static liquefaction is likely the most common.

Recent tailing storage facilities (TSF) failures have highlighted the brittleness of the materials deposed in these geotechnical structures – dams or piles - and emphasized the importance of studying this peculiar material in order to understand their mechanical behaviour and designing safer TSF, herein with emphasis to tailing dams. Although the structure design plays a main role, the nature of the tailings itself make this material particularly sensitive to instability by liquefaction triggering. The characteristics of this type of material are highly influenced by its man-made origin. The fact that tailings are generated by crushing and processing of a parent rock, not subject to chemical weathering, explains its low or non-existing plasticity and the small particle size (predominantly silty or sandy-silty) and high-water content turns them liquefiable.

In this study, the mechanical behaviour of a silty-sand iron tailing from Brazil is explored in the light of critical state soil mechanics. The tailing material was collected from a large scale tailing dam in Minas Gerais where the upstream construction method was employed. Strain softening and static liquefaction are often considered the triggering factors for the failures of loose granular slopes. These triggering mechanisms have been extensively studied over the years. Still, much of the data deals with granular soils, considerable effort has been devoted to understanding the undrained behaviour of tailing materials using the triaxial apparatus as reference (eg.: Bedin et al. 2012; Soares & Viana Da Fonseca 2016; Morgenstern et al. 2016; Robertson et al.) These studies have not always been consistent, as there is no unified framework, which links all aspects full response mechanisms in tailings.

To extend this knowledge, an experimental testing programme was carried out with the aim of studying the behaviour of a silty-sand iron tailings from mines in Brazil, in the light of critical state soil mechanics and evaluating the instability behaviour under undrained conditions. Instability is here defined as a phenomenon that triggers the development of large strains, corresponding to a strain-softening behaviour accompanied by increasing pore pressures and a reduction in deviatoric stresses (Kramer 1996). In extreme conditions this can lead to a complete loss of shear strength, experiencing true liquefaction. This instability process, as described in Gens (2019) takes place when the deviator stress reaches the value of peak strength. In these conditions there is an apparent inconsistency. When an undrained test reaches its peak strength, the material softens and collapses, especially under stress-controlled conditions. This paradox is usefully explored using the important concept of controllability developed by Professor Roberto Nova and co-workers (cited by Gens 2019). Ramos et al. (2015) have presented a comprehensive work on modelling flow instability of an Algerian sand with the dilatancy rule in a modified version of the CASM model (Yu 1996). The CASM model, implemented in Code_Bright (Technical University of Catalonia, UPC) has been selected because: it is relatively simple having a single yield surface; it is based on the state parameter concept; it uses non-associated plasticity allowing for instability phenomena to be reproduced; and, selecting appropriate parameters, it can mimic classical critical state models. The critical state parameters were defined in the geotechnical laboratory in UPorto by a series of triaxial tests (two under drained and six under undrained conditions) with different initial confining pressures on Les Dunes sand, Alger. CASM is implemented in Code_Bright, the code used to obtain the numerical solutions of these triaxial tests. The material parameters were calibrated based on the experiments simulated. In that paper a singular test was simulated, where a sand specimen was first submitted to drained condition and then, at an intermediate loading level, the condition changed to undrained, i.e., the water flux in the specimen stops, was conducted to evaluate the sensibility of this model to detect the triggering of instability. In Figure 1 the stress-paths for several simulations are represented. In each, the drained process was stopped at different times. The critical state line and the instability line are also represented, with the intention of being reference lines. The stress-path for 250 hours represents the fully drained test. All tests performed follow the drained path until the moment they start to be undrained.

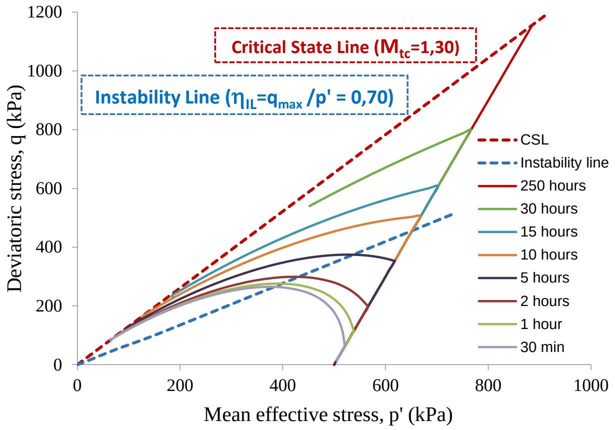

Figure 1. Stress-paths of drained-undrained simulations (Ramos et al. 2015)

Ramos et al. (2015) concluded that the instability line in this sand is a straight line, passing in the peak of deviatoric stress in q-p′ space, for the undrained tests. According to this criterion, a specimen under drained conditions is never unstable. A specimen loaded in undrained conditions may become unstable, after its stress-path crosses the instability line and enters the region of potential instability. Instability was confirmed in the simulation of drained-undrained tests, these tests starting to be drained and at different times the conditions were changed to undrained. If the undrained conditions start when the stress-path has already crossed the instability line, the specimen may already be unstable, while, if a test starts to be undrained before reaching the instability line, it stays stable only when the undrained stress-path crosses the instability line, that is when the second order work increment is zero, instability may occur.

In this paper, most of the work is concentrated on undrained tests because static/flow instability (cause by either strain softening or liquefaction) is triggered by undrained failure in monotonic shear. The results from the laboratory testing programme to evaluate the behaviour of the iron tailing are here presented and interpreted in the critical state framework. Drained and undrained triaxial tests sheared under monotonic loading allowed the definition of the CSL. The non-linear shape observed in the CSL was used to investigate the intrinsic dynamics of the monotonic undrained response of tailings and to define the instability locus. The undrained behaviour of the tailing was studied by performing a series of anisotropically consolidated undrained tests

that better replicate the stress state in situ, for a range of mean effective consolidation stresses and void ratios.

2 MATERIALS AND METHODS

2.1 *Material Properties*

The tailing material presented in this paper was collected from one of the hundred tailings dams located in Minas Gerais, an inland state in the Southeast of Brazil. The silty sand iron tailing in this study was tested in its “natural” or in-situ grading. A large composite bulk was first created by combining and thoroughly mixing all the material collected in order to guarantee the homogeneity of the tested material.

The physical properties of the soil are summarized in Table 1 and particle size distribution presented in Figure 3. The material is non-plastic, predominantly sand-sized, with a specific gravity of 4.994, an uncommonly high value but consistent with tropical iron-rich laterite soils originated from a miner exploitation.

Scanning electron microscopy (SEM) and X-ray diffraction (XRD) were also completed to determine the typical particle shapes and the main mineral constituents, respectively. The SEM images of the particles and analysis quantifying the mineral composition are presented in Figure 3.

Table 1. Physical properties of the studied soil

Parameter	Value	Unit
Specific Gravity, G_s	4.994	-
Mean Particle Size, D_{50}	0.093	mm
Fines Content, FC	36.49	%
Coefficient of Curvature, C_c	1.18	-
Coefficient of Uniformity, C_u	3.18	-
Maximum Void Ratio, e_{max}	1.22	-
Minimum Void Ratio, e_{min}*	0.48	-
Particle Shape	Sub-rounded to angular	-

Note: Minimum and maximum densities were determined by Japanese Geotechnical Society standard (JGS-0161 2009); Ishihara et al. (2016) correction to sandy soils with fines higher than 5% for e_{min}* was applied.

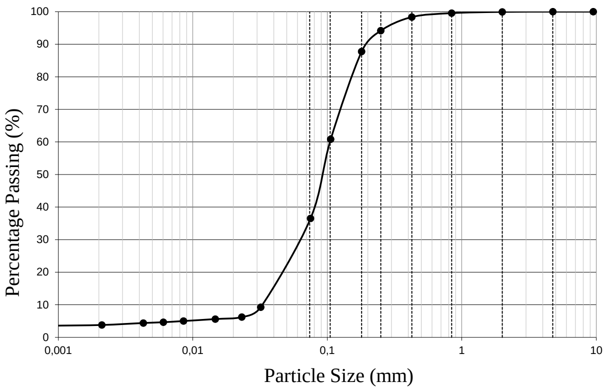

Figure 3. Particle size distribution of the silty-sand iron tailing

The remoulded samples were prepared using the moist tamping technique simultaneously with the undercompaction method (Ladd 1978), as it allows to produce uniform and reproducible soil specimens with very loose conditions. Loose samples are selected to minimize the potential of shear localisation and specimen non-uniformity from affecting the results, ensuring a reliable measurement of the CSL.

For critical state assessment, the samples were 70 mm in diameter with an initial height-to-diameter ratio of $H/D \approx 2$. The specimens were fully saturated until the Skempton's B value >0.98 was reached, by flushing CO_2 and de-aired water, back-pressure increments and additional percolations under pressure. The saturation process is fundamental for a proper assessment of the CSL, as the constant volume (or undrained) conditions cannot be assumed unless the soil is fully saturated.

The samples were then isotropically consolidated and sheared

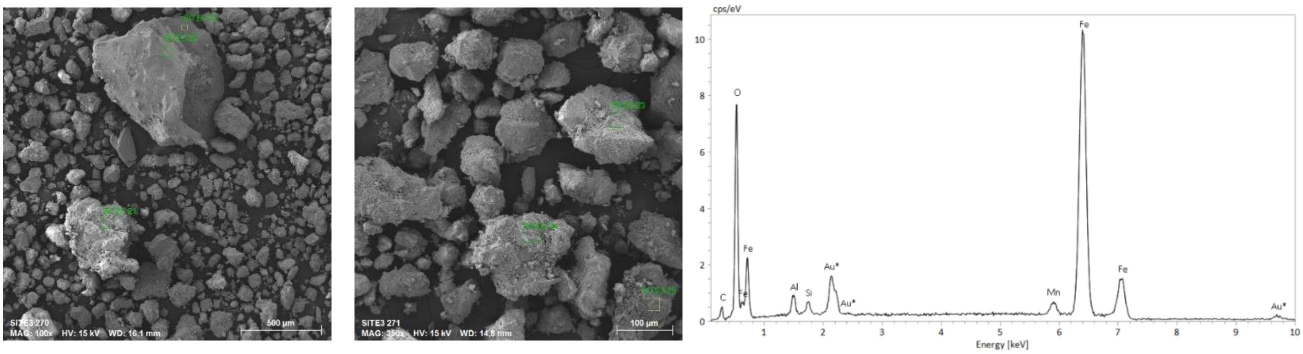

a. b. c.

Figure 2. Scanning electron microscopy and X-ray diffraction of the silty-sand iron tailing: a. SEM image (horizontal bar corresponds to 500μm); b. SEM ((horizontal bar corresponds to 100μm); c. EDS spectrum

The identified iron as the main component with small percentages of gold (his coming from the thin layer sputtered on the samples for conductivity purposes), aluminium and silicon. The morphology from the SEM tests indicates a granulometric variability, with the presence of small fibrous particles attached to larger particles, and a sub-angular to angular shape.

2.2 *Testing Procedures*

The experimental programme in the laboratory was divided in two phases: i) the definition of the iron tailing critical state line; ii) the analysis of the undrained behaviour of the material; using the triaxial apparatus as reference. Two different equipment configurations were used. The first configuration corresponds to triaxial cells with lubricated end platens and an embedded top cap loading ram connection, to perform conventional isotropically consolidated drained and undrained triaxial tests to define the CSL. The second configuration is a Bishop-Wesley stress path type-automatic controlled triaxial cell, that allows advanced testing to study the undrained behaviour of the soil. All tests were sheared under monotonic loading.

In this paper, the term "triaxial test" will be used do designate the tests executed in the lubricated end chambers to infer the critical state line, and the term "stress-path tests" to represent the tests carried out in the Bishop-Wesley cell to access the undrained response of the material.

2.2.1 *Triaxial Tests*

For the triaxial tests, the samples were tested in conventional triaxial apparatus provided with oversized lubricated end platens and an embedded top-cap loading ram connection. The implementation of these improvements in the triaxial apparatus results in a uniform shearing without the generation of spurious shear bands, allowing a reduction of strain softening and the stabilisation of volumetric strain, which are determinant factors for the identification of the CSL (Viana da Fonseca et al. 2021).

under conventional drained or undrained conditions. The end-of-test soil freezing technique was employed after shearing, because of its precision and simplicity of void ratio measurement through the final gravimetric water content.

In the data analysis there was no need to correct the membrane penetration effect due to the soil small particles size, however the membrane rigidity affects the results, specially at low confining pressures. To correct the stresses, the formulae suggested by Duncan & Seed (1967) was used for both triaxial and stress-path tests. Details regarding sample preparation, improvements in the triaxial apparatus and testing methods used in this programme can be consulted in Viana da Fonseca et al. (2021).

The list and details of the triaxial tests performed to define the critical state line are given in Table 2.

Table 2. Summary of the triaxial tests

Test No.	Test Type	e_0	p'_0 (kPa)	Shearing
1	CID	1.21	50	Strain Control
2	CID	1.27	100	Strain Control
3	CID	1.28	200	Strain Control
4	CID	1.26	400	Strain Control
5	CID	1.27	800	Strain Control
6	CID	1.27	1600	Strain Control
7	CIU	1.25	800	Strain Control

Note: CID and CIU, isotropically consolidated drained and undrained test, respectively; e_0, initial void ratio: p'_0, mean effective consolidation stress.

2.2.2 *Stress Path Tests*

A proper consideration of the undrained behaviour should rely on tests that adopt the initial stress state representative of the in-situ conditions (K_0) and specific stress loading paths occurring in the geotechnical structures. For this purpose, fully automated Bishop-Wesley triaxial cells were used allowing a numerous loading strain and stress paths.

The samples were remolded using the same techniques describe above, as it allows to remould very loose samples and thus consequently to investigate instability conditions. For stress-path tests, the samples were 50 mm in diameter with an initial height-to-diameter ratio of $H/D \approx 2$. A full saturation condition with B-values higher than 0.98 was achieved applying the same procedures as in the tests performed to reach ultimate critical state. The importance of full saturation is even more pronounced in undrained tests since the development of pore-water pressure strongly depends on the stiffness of the pore fluid. The samples were anisotropically consolidated under a $K_0 \approx 0.5$ and sheared under undrained strain paths. The void ratio was determined by the direct measurement of end-of-test gravimetric water content, as freezing was not compatible with the equipment.

The list and details of the triaxial tests performed to access the undrained behaviour are given in Table 3.

Table 3. Summary of the stress-path tests

Test No.	Test Type	e_0	p'_0 (kPa)	Shearing
8	CKU	1.30	200	Strain Control
9	CKU	1.30	400	Strain Control
10	CKU	1.29	800	Strain Control
11	CKU	1.03	200	Strain Control
12	CKU	0.96	400	Strain Control

Note: CKU, anisotropically consolidated undrained test; e_0, initial void ratio: p'_0, mean effective consolidation stress

3 RESULTS

3.1 *Critical State Line*

All samples listed in Table 3 exhibited contractive behaviour, each achieving critical state conditions with negligible changes in stress, volume change and/or shear induced pore pressure. The ultimate state was reached for around 30% of axial strain. From Figure 4a, it can be observed that all endpoints define a unique CSL in the *q:p'* space, which is clearly represented by a straight line passing through the origin (linear fit). However, in the *e:log p'* plane (Figure 4b), the critical state points exhibit sufficient curvature for the CSL to be projected through a "power law" formulation as proposed by Li and Wang (1998). The inferred critical state parameters are presented in Table 4.

CSSM framework states that CSL corresponds to a straight line in both *q:p'* and *e:log p'* spaces. However, several authors (e.g.: Li & Wang 1998; Verdugo & Ishihara 1996) recognise that in granular materials a curve, with the form of the power-law $e = A + B(p'/100)^C$, provides a best fit to represent the CSL in the e:log p' space. This curvature in the CSL in mainly related to flow instabilities at low stress levels and grain changes induced at higher stress-states (Carrera et al. 2011; Schnaid et al. 2013; Soares & Viana da Fonseca 2016).

Particle size distribution (PSD) analysis of the specimens at the end of the shear stage revealed that PSD does not change after testing, showing that there is no significant breakage of particles of the iron tailing. The non-linearity of the CSL for higher pressures cannot be attributed to particle breakage, however there may be an evolution of the morphology of the particles, not in size but in shape (e.g.: convexity, circularity, roundness and sphericity), that would require advanced analysis. There is no fundamental physical framework linking microscopic phenomena to macroscopic behaviour, and, for this reason, the discussion presented herein is speculative and conceived to provide a basis for future ongoing research.

For lower stresses states, the CSL tends to a horizontal asymptote as p' reduces. This is a consequence of flow instabilities, which in many cases leads to soil liquefaction in contractive materials under undrained conditions. This curved critical state line gives rise to an increased susceptibility to liquefaction, supporting the investigation of the intrinsic dynamics of the monotonic undrained response of tailings.

Table 4. Inferred critical state parameters

Linear fit $q = M_c \cdot p'$		Power-law fit $e_{cs} = A - B \cdot (p'/100)^C$		
M_c	φ'_{cs} (°)	A	B	C
1.366	33.80	1.078	0.023	0.705

Note: M_c is the is the slope of critical state locus in *p':q* plane; φ'_{cs}, is the critical state friction angle.

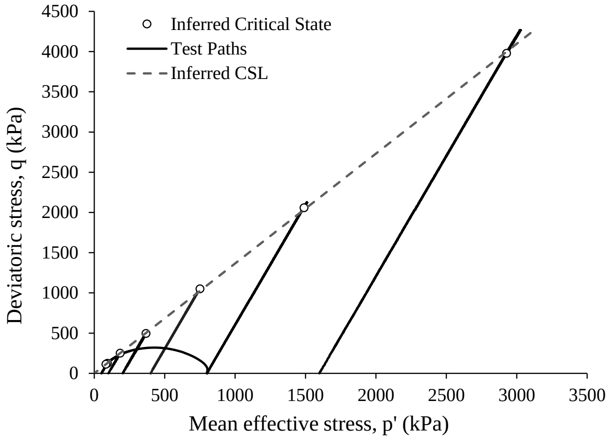

a)

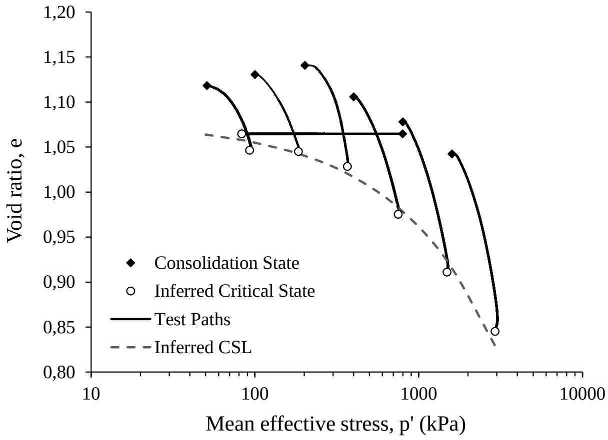

b)

Figure 4. Inferred CSL on the: a) *q:p'* invariant space; b) *e:log p'* invariant space.

3.2 *Undrained Behavior*

3.2.1. *Instability Mechanisms*

The schematic stress and strain paths in Figure 5 represent different types of undrained behaviour typically observed on granular soils. For some combinations of density and stress levels, undrained shearing from a state that is initially above the CSL, in *e-log p'* space, exhibit a strain hardening compressive behaviour towards critical state with a sustained increase of pore pressure, as represented in stress path (iii). This seems often to be the case at higher stress levels when samples are sheared to more linear part of the CSL. For other conditions, undrained shearing on a loose specimen will present a strain-softening compressive behaviour, followed by a loss of stability, rapid increase in shear strains and uncontrolled pore pressure development that can lead to uncontrollable failure. Once the deviatoric stress reaches a peak (q_{max}), the undrained shear strength reduces and the material softens afterwards [stress path (ii)]. This behaviour can be even more pronounced, as represented in stress path (i) where the pore pressure equals the cell pressure, and therefore p' and q tend to zero. This should be termed true or complete liquefaction. These two instability mechanisms (strain-softening and liquefaction) will be distinguished accordingly to Yamamuro & Covert (2001). As represented in Figure 5, the stress-path (ii) suffers a severe strain softening but no liquefaction (some name it as "partial" liquefaction") as it reaches a stable critical state, while stress-path (i) has genuinely reached a liquefied state, with zero effective stress and zero strength. The term instability is used here to describe a runway deformation that occurs due to the inability of a soil specimen to sustain a given load or stress.

Furthermore, undrained shearing from a state that is initially bellow the CSL is represented in stress-path (iv). Dense samples will present an initial contractiveness due to the increase of pore pressure. However, as the effective stress-path crosses the phase transformation line, the supressed dilation produces negative increment of pore pressure and the effective stress path moves towards higher effective confining pressures and deviatoric stresses. This stable behaviour continues until a steady-state (critical) point is reached.

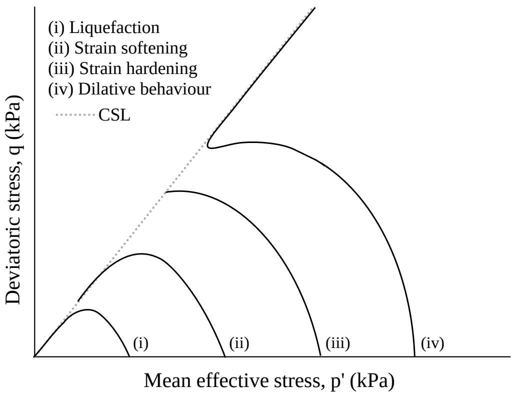

a)

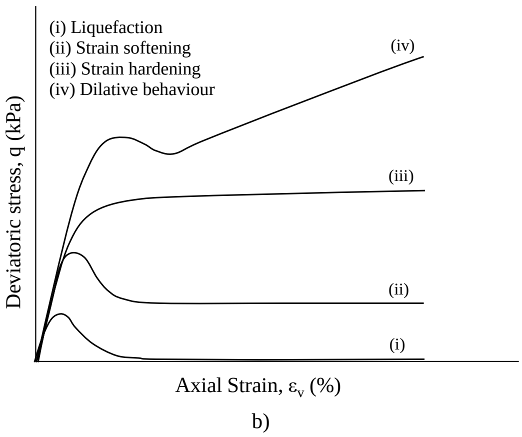

b)

Figure 5. Schematic diagrams of four possible different patterns of behavior associated with undrained loading: a) typical stress paths; b) deviatoric stress evolution

3.2.2. *Instability Locus of the Iron Tailings*

Figure 6 presents the stress paths of the tests performed to access the undrained behavior, in the *q:p'* plane. In this series of undrained tests, all loose samples exhibit positive pore water pressure, revealing the tendency to contractive response over a wide range of confining pressures. The generated excess pore pressure shows a smooth increase during shear, with no identifiable inflection point that might indicate a collapsible response associated with a meta-stable rearrangement of soil particles. Tests 9 and 10 suffered severe strain softening but with no liquefaction, as a stable critical state is reached. In Test 8, true liquefaction is developed, with the annulment of the mean effective stress and deviator stress. The q_{max} points for those samples who experienced instability mechanisms allowed the definition of the instability line (IL) in the *q:p'*. The undrained stress-path of test 7 was also added to validate the instability locus between isotropic and anisotropic consolidated specimens. The instability region is then limited between the CSL and the IL. The stress ratios (*q*/*p*') of the two linear loci (M_c for the CSL and η_{IL} for the IL) are defined in Figure 6.

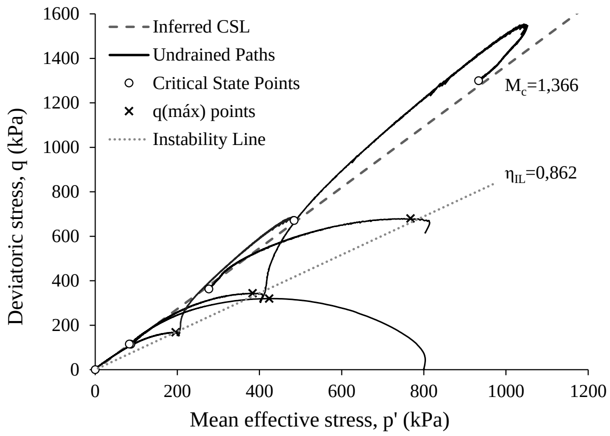

Figure 6. Stress paths and instability locus (line) from undrained monotonic shear tests of the silty-sand iron tailing

The position of the undrained tests was plotted and compared to CSL location in Figure 7. As stated by Carrera et al. (2011) and Yamamuro & Covert (2001), not all samples whose state is above the CSL reach true liquefaction, only those whose initial state lies above the horizontal asymptote of the CSL, which for an undrained shearing generates an annulment of the effective confinement stress, *p'*. Therefore, susceptibility to true static liquefaction primarily depends more on the initial void ratio of the soil than on the stress state.

Figure 7 also presents a suggested subdivision of the area above the CSL into three different regions with different behaviours. The liquefaction zone is limited by e_{liq}, the void ratio corresponding to the horizontal asymptote of the CSL. All specimens at higher void ratios than e_{liq} must liquify too. Similar behaviour was obtained in previous studies on gold tailings (Bedin et al. 2012; Schnaid et al. 2013). The strain softening zone is located on the curved part of the CSL. The specimens will suffer severe strain softening but will not liquify, reaching a stable state. The strain hardening region was extrapolated from the linear part of the CSL. No test was presented with strain hardening behaviour, as it would require advanced high-pressure tests, as included in the results with other granular materials presented in Soares & Viana Da Fonseca (2016).

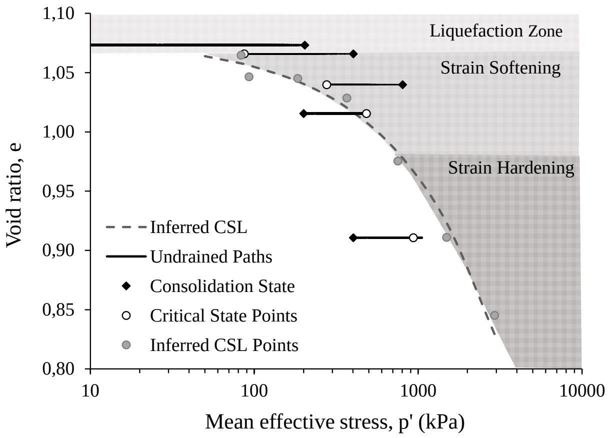

Figure 7. Undrained behavior in *e : log p'* plane (based on Carrera et al. 2011)

As for the dense samples, a stable behaviour was observed. The samples exhibit little contractiveness, generating negative pore pressure which increased the effective stresses and strength. Test 11 presented a dilative strain hardening behaviour while test 12 revealed a a dilative strain softening tendency. However, it was observed shear localisation in this sample, justifying the non-homogeneous stresses and strains.

4 CONCLUSIONS

An experimental testing programme was carried out with the aim of studying the behavior of a silty-sand iron tailing in the light of critical state soil mechanics and evaluating the instability locus under undrained conditions.

The critical state of the iron tailing was shown to be highly non-linear, reflecting flow instability of the tailings structure for lower stress levels, as well as possible changes in grain shape (morphology) induced by crushing at high mean stresses.

In studying the undrained behaviour of the soil was stated that true liquefaction cannot be reached by all samples whose state is above the CSL, but only by those samples whose initial state lies above the horizontal asymptote of the CSL. Therefore, susceptibility to true static liquefaction depends on the initial void ratio of the soil but not on the stress state. Three classes of behavior were identified related to the void ratio:

a) Liquefaction region: this region occurs above the horizontal asymptote of the CSL, limited by e_{liq}. These tailings present large inherent contractiveness that causes complete liquefaction.
b) Strain softening region: located in the curve part of the CSL. Effective stress paths indicate a brief drop in the stress difference after reaching an initial peak value. The sample will present strain softening without true liquefaction.
c) Strain hardening region: located at the linear part of the CSL, the samples will reach stable critical states, presenting a compressive behavior.

Undrained softening (without reaching zero strength) leads to large deformations and can also lead to flow liquefaction and, consequently to catastrophic occurrences, highlighting the importance on the investigation of the undrained behavior in mining tailings. A special attention has to be made to high pressure confinements. An experimental research program is being developed in the university of Porto in tailing produced in Brazilian iron mines.

5 ACKNOWLEDGEMENTS

This work in FEUP was financially supported by: Base Funding – UIDB/04708/2020 of the CONSTRUCT – Institute of R&D in Structures and Construction funded by national funds through the FCT/MCTES (PIDDAC). The SEM and XRD analysis were carried out by Professor Isabel Fernandes in the Faculty of Sciences of University of Lisbon, to whom the authors are truly grateful.

6 REFERENCES

Bedin, J., F. Schnaid, A. V. da Fonseca, and L. M. de Costa Filho. 2012. “Gold Tailings Liquefaction under Critical State Soil Mechanics.” *Geotechnique*. Thomas Telford Ltd . https://doi.org/10.1680/geot.10.P.037.

Carrera, A., M. Coop, and R. Lancellotta. 2011. “Influence of Grading on the Mechanical Behaviour of Stava Tailings.” *Geotechnique* 61 (11): 935–46. https://doi.org/10.1680/geot.9.P.009.

Carrier, W. D. 2003. “Stability of Tailing Dams.” In *XIX Conference of Geotechnics of Turin on Slope Stability and Stabilization*. Turin, Italy.

Duncan, J. M., and H. B. Seed. 1967. “Corrections for Strength Test Data.” *Journal of the Soil Mechanics and Foundations Division* 93 (5): 121–37. Accessed June 1, 2021. https://doi.org/10.1061/JSFEAQ.0001015.

Gens, A. 2019. “Hydraulic Fills with Special Focus on Liquefaction.” In *17th European Conference on Soil Mechanics and Geotechnical Engineering, ECSMGE 2019*. 52–82. doi: 10.32075/17 ECSMGE-2019-1108.

Ishihara, K., K. Harada, W. F. Lee, C. C. Chan, and A. M. M. Safiullah. 2016. “Post-Liquefaction Settlement Analyses Based on the Volume Change Characteristics of Undisturbed and Reconstituted Samples.” *Soils and Foundations* 56 (3): 533–46.

Japanese Geotechnical Society. 2009. *JGS 0161 - Test Method for Minimum and Maximum Densities of Sands*.

Kramer, S. L. 1996. *Geotechnical Earthquake Engineering*. Prentice-Hall, New Jersey.

Li, X. S., and Y. Wang. 1998. “Linear Representation of Steady-State Line for Sand.” *Journal of Geotechnical and Geoenvironmental Engineering* 124 (12): 1215–17. https://doi.org/10.1061/(asce)1090-0241(1998)124:12(1215).

Morgenstern, N. R., S. G. Vick, C. B. Viotti, and B. D. Watts. 2016. “Fundão Tailings Dam Review Panel: Report in the Immediate Causes of the Failure of the Fundão Dam.” New York.

Ramos, C., A. Viana, D. Fonseca, J. Vaunat, and A. Viana Da Fonseca. 2015. “Modeling Flow Instability of an Algerian Sand with the Dilatancy Rule in CASM LIQUEFACT View Project Proyecto PROGRESS-CEE View Project Modeling Flow Instability of an Algerian Sand with the Dilatancy Rule in CASM.” *Geomechanics and Engineering* 9 (6): 729–42. https://doi.org/10.12989/gae.2015.9.6.729.

Robertson, P. K., L. de Melo, D. J. Williams, and W. Wilson. n.d. “Report of the Expert Panel on the Technical Causes of the Failure of Feijão Dam I.” Accessed June 1, 2021; http://www.b1technicalinvestigation.com/.

Schnaid, F., J. Bedin, and L. M. Costa Filho. 2007. “Piezocone in Silty Tailing Materials.” *Studia Geotechnica et Mechanica* Vol. 29 (nr 1-2): 151–62.

Schnaid, F., J. Bedin, A. J. P. Viana da Fonseca, and L. de Moura Costa Filho. 2013. “Stiffness and Strength Governing the Static Liquefaction of Tailings.” *Journal of Geotechnical and Geoenvironmental Engineering* 139 (12): 2136–44. https://doi.org/10.1061/(asce)gt.1943-5606.0000924.

Soares, M., and A. Viana Da Fonseca. 2016. “Factors Affecting Steady State Locus in Triaxial Tests.” *Geotechnical*

Testing Journal 39 (6): 1056–78. https://doi.org/10.1520/GTJ20150228.

Verdugo, R., and K. Ishihara. 1996. "The Steady State of Sandy Soils." *Soils and Foundations* 36 (2): 81–91. https://doi.org/10.3208/sandf.36.2_81.

Viana da Fonseca, A., D. Cordeiro, and F. Molina-Gómez. 2021. "Recommended Procedures to Assess Critical State Locus from Triaxial Tests in Cohesionless Remoulded Samples." *Geotechnics*. ID: 1280000 (MDPI: ISSN: 2673-709)

Yamamuro, J. A., and K. M. Covert. 2001. "Monotonic and Cyclic Liquefaction of Very Loose Sands with High Silt Content." *Journal of Geotechnical and Geoenvironmental Engineering* 127 (4): 314–24. https://doi.org/10.1061/(asce)1090-0241(2001)127:4(314).

Yu, H. S. 1996. "CASM: A Unified State Parameter Model for Clay and Sand." *International Journal for Numerical and Analytical Methods in Geomechanics,* 22(8), 621-653. Doi: 10.1002/(SICI)1096-9853(199808).